Research Article

Journal of PeptideScience

Received: 18 August 2010 Revised: 15 October 2010 Accepted: 16 October 2010 Published online in Wiley Online Library: 3 February 2011

(wileyonlinelibrary.com) DOI 10.1002/psc.1328

DPP-IV-resistant, long-acting oxyntomodulin derivatives

Alessia Santoprete,[a,b] Elena Capitò,[a,c] Paul E. Carrington,[d] Alessandro Pocai,[d] Marco Finotto,[a] Annunziata Langella,[a,e] Paolo Ingallinella,[a,f] Karolina Zytko,[a] Simone Bufali,[a,g] Simona Cianetti,[a,g] Maria Veneziano,[a] Fabio Bonelli,[a,b] Lan Zhu,[d] Edith Monteagudo,[a,b] Donald J. Marsh,[d] Ranabir SinhaRoy,[d] Elisabetta Bianchi[a,b] and Antonello Pessi[a,h]*

Obesity is one of the major risk factors for type 2 diabetes, and the development of agents, that can simultaneously achieve glucose control and weight loss, is being actively pursued. Therapies based on peptide mimetics of the gut hormone glucagon-like peptide 1 (GLP-1) are rapidly gaining favor, due to their ability to increase insulin secretion in a strictly glucose-dependent manner, with little or no risk of hypoglycemia, and to their additional benefit of causing a modest, but durable weight loss. Oxyntomodulin (OXM), a 37-amino acid peptide hormone of the glucagon (GCG) family with dual agonistic activity on both the GLP-1 (GLP1R) and the GCG (GCGR) receptors, has been shown to reduce food intake and body weight in humans, with a lower incidence of treatment-associated nausea than GLP-1 mimetics. As for other peptide hormones, its clinical application is limited by the short circulatory half-life, a major component of which is cleavage by the enzyme dipeptidyl peptidase IV (DPP-IV). SAR studies on OXM, described herein, led to the identification of molecules resistant to DPP-IV degradation, with increased potency as compared to the natural hormone. Analogs derivatized with a cholesterol moiety display increased duration of action *in vivo*. Moreover, we identified a single substitution which can change the OXM pharmacological profile from a dual GLP1R/GCGR agonist to a selective GLP1R agonist. The latter finding enabled studies, described in detail in a separate study (Pocai A, Carrington PE, Adams JR, Wright M, Eiermann G, Zhu L, Du X, Petrov A, Lassman ME, Jiang G, Liu F, Miller C, Tota LM, Zhou G, Zhang X, Sountis MM, Santoprete A, Capitò E, Chicchi GG, Thornberry N, Bianchi E, Pessi A, Marsh DJ, SinhaRoy R. Glucagon-like peptide 1/glucagon receptor dual agonism reverses obesity in mice. *Diabetes* 2009; 58: 2258–2266), which highlight the potential of GLP1R/GCGR dual agonists as a potentially superior class of therapeutics over the pure GLP1R agonists currently in clinical use.

Keywords: oxyntomodulin; GLP-1 receptor agonists; GLP-1/glucagon receptor dual agonists

Introduction

Obesity is one of the major risk factors for type 2 diabetes, and the development of agents, that can simultaneously achieve glucose control and weight loss, is being actively pursued. Therapies based on peptide mimetics of the gut hormone glucagon-like peptide 1 (GLP-1) are rapidly gaining favor, due to their ability to increase insulin secretion in a strictly glucose-dependent manner, with little or no risk of hypoglycemia [1–3]. As a highly beneficial feature, GLP-1 peptide mimetics also cause a modest, but durable weight loss in patients with type 2 diabetes. On the basis of the effects of incretin-based therapies, much interest is focused on the evaluation of other peptides from the glucagon (GCG) family, including oxyntomodulin (OXM).

OXM, a 37-amino acid peptide hormone that is a product of the proglucagon gene, is secreted post-prandially by the L-cells in the small intestine. It shows sequence homology with both GCG and GLP-1 (Figure 1). Unlike GLP-1 that shows activity only on the GLP-1 receptor (GLP1R), OXM has dual agonistic activity on both the GLP1R and the GCG receptor (GCGR) albeit with 10–100-fold reduced potency compared to the cognate ligands, GLP-1 and GCG [4–6]. Modulation of glucose and energy homeostasis by OXM has been shown to depend on GLP1R activation but other mechanisms of OXM pharmacology are less well understood [7–9].

* *Correspondence to: Antonello Pessi, PeptiPharma, Via dei Castelli Romani 22, 00040 Pomezia (RM), Italy. E-mail: a.pessi@peptipharma.it*

a *Istituto di Ricerche di Biologia Molecolare P. Angeletti, 00040 Pomezia, Rome, Italy*

b *IRBM Science Park, Via Pontina km 30,600, 00040 Pomezia (RM), Italy*

c *BASF, Via Pila 6, 40037 Pontecchio Marconi (BO) Italy*

d *Merck Research Laboratories, Rahway, NJ 07065, USA*

e *Merck Serono S.p.A. DSD Department, Via Luigi Einaudi, 11, 00012 Guidonia Montecelio, Rome, Italy*

f *Diasorin Research Center c/o Insubrias BioPark, Via R. Lepetit 34, 21040 Gerenzano (Varese), Italy*

g *Novartis Research Laboratories, Novartis Vaccines and Diagnostic, Via Fiorentina 1, 53100 Siena, Italy*

h *PeptiPharma, Via dei Castelli Romani 22, 00040 Pomezia (RM), Italy*

Journal of PeptideScience

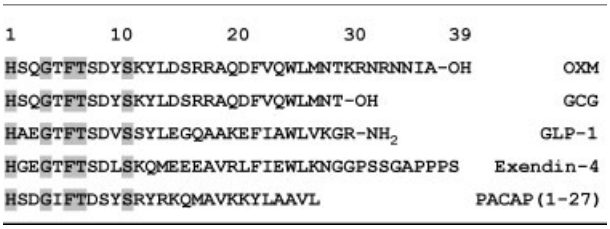

Figure 1. Primary structure of OXM, GCG, GLP-1, exendin-4, and pituitary adenylate cyclase activating peptide 1–27 (PACAP 1–27). The *N*-terminal residues conserved among all peptides are highlighted in gray.

Acute and chronic administration of OXM can reduce food intake in rodents [10,11]. In a 4-week study in humans, peripheral administration of OXM was shown to reduce food intake and body weight by 1.9% relative to the control group [12]. In a separate 4-day study also in humans, OXM also increased energy expenditure and physical activity levels [13]. Notably, unlike treatments with GLP-1 analogs for which dose-limiting nausea and vomiting has been reported in a majority of patients, in both human studies a low incidence of nausea was associated with OXM treatment. Thus, OXM is one of the few obesity targets with both, human validation and an attractive tolerability profile.

As for other peptide hormones, the clinical application of native OXM is limited by its short circulatory half-life [14]. After secretion of OXM, circulating levels are rapidly cleared by the action of dipeptidyl peptidase IV (DPP-IV) which inactivates OXM by removing the His–Ser dipeptide from the *N*-terminus [15]. As is the case with GLP-1, the cleaved peptide OXM(3–37) has no agonist activity.

Recently Druce *at al*. reported SAR studies of OXM, leading to the design of lipidated analogs that reduced food intake up to 24 h post dosing in mice [16]. Although an important step in the development of OMX-based therapeutics, their studies did not address two key questions, which are critical to understand the potential advantages and disadvantages of therapeutics with a dual GLP1R/GCGR agonist profile, such as OXM, *versus* the clinically validated pure GLP-1 agonists such as exenatide [1] and liraglutide [3]. Firstly, what is the relative contribution of GLP1R and GCGR agonism to the anti-obesity effect of OXM? Secondly, what is the effect of the simultaneous activation of GLP1R and GCGR on glucose control?

These questions are made more important by the recent report that a long-acting GLP1R/GCGR co-agonist is a particularly efficacious anti-obesity agent, without any overt signs of adverse effects [17].

SAR studies on OXM, which led us to identify amino acid substitutions that differ from those reported by Druce *et al*., are reported here. These novel mutations confer complete resistance to DPP-IV cleavage, while preserving or even enhancing the agonist activity at both GLP-1 and GCG receptors. Moreover, it is demonstrated that a single amino acid change can switch the pharmacological profile of OXM analogs from a dual GLP1R/GCGR agonist to a pure GLP-1 agonist. Finally, we have developed long-acting analogs by addition of a cholesterol group at a suitable position in the OXM sequence. Use of short- and long-lived 'matched pairs' derived from this SAR enabled the question of dual *versus* GLP1R-selective agonism, to be addressed in the absence of confounding effects that arise from differences in bioavailability, absorption and metabolic stability of the components of the 'matched pair'.

Table 1. List of OXM analogs with modifications at the *C*- or *N*-terminus

Compound	Peptide[a]	EC_{50} (nM) on GLP1R −DPP-IV	EC_{50} (nM) on GLP1R +DPP-IV	EC_{50} (nM) on GCGR
1	OXM	7.0	>200	5.7
2	GCG	na[b]	na	0.07
3	OXM-NH_2	9.2	>200	5.5
4	Pyr-OXM-NH_2	77	541	>200
5	Ac-OXM-NH_2	>200	>200	>100
6	Bzl-OXM-NH_2	92	63	2.6
7	Bz-OXM-NH_2	43	73	28
8	PEG_4-OXM-NH_2	265	1031	>700
9	Imi-H-OXM-NH_2	24	21	24
10	Me-H-OXM-NH_2	64	36	46
11	Me_2-H-OXM-NH_2	268	236	>1000
12	ΔNH_2-H-OXM-NH_2	27	31	54

Agonist potency *in vitro* against GLP1R, with and without pre-incubation with DPP-IV, and against GCGR.
[a] Bzl, benzyl; Bz, benzoyl; PEG_4, CH_3-O-$(CH_2$-CH_2-$O)_3$-CH_2-CH_2-CO-; imi-H, imidazol-lactyl; Me-H, *N*-methyl-His; Me_2-H, *N*,*N*-dimethyl-His; ΔNH_2-H, desamino-His.
[b] na, not active

A separate manuscript [18] reported the results of a detailed investigation with OXM matched pair peptides, which concluded that in a rodent model of obesity dual GLP1R/GCGR agonists can lower blood glucose, reduce food intake, and decrease body weight with prolonged duration of action and sustained efficacy with respect to equipotent GLP1R-only agonists, at equivalent doses and exposures, without a concomitant increase in the risk of hyperglycemia.

Results and Discussion

Stabilization Against Enzymatic Cleavage

Figure 1 shows the primary sequence of OXM in comparison with GLP-1 and GCG. Also shown are the sequences of exendin-4, a potent, selective GLP1R agonist in clinical use for type 2 diabetes [1], and pituitary adenylate cyclase-activating peptide (PACAP), which does not bind either GLP1R or GCGR, but shares considerable sequence homology with GLP1R/GCGR agonists in the *N*-terminal region, and is the only type B GPCR-binding hormone for which the structure of the *N*-terminal region has been determined in complex with the receptor [19].

Modifications of the C-terminus

Replacement of the *C*-terminal carboxylate of OXM (sequence shown in Figure 1) with an amide stabilized the peptide against carboxypeptidases, and demonstrated that the *C*-terminal carboxylate is not essential for activity on either GLP1R or GCGR (compare **1** and **3** in Table 1). Therefore, most of the subsequent analogs were produced with a *C*-terminal amide.

Modifications of the N-terminus

DPP-IV is the main enzyme involved in the inactivation of many peptide hormones, including GLP-1 and OXM. Mutations that

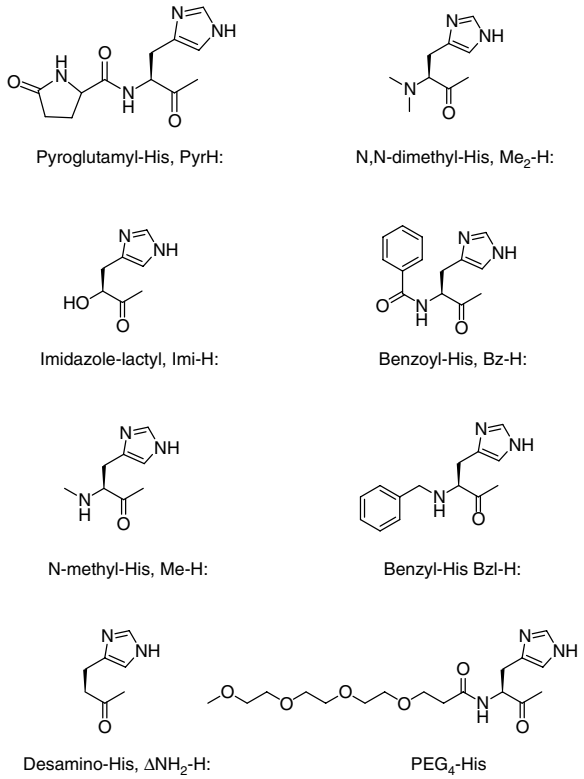

Figure 2. Structure of the capping groups used in Table 1.

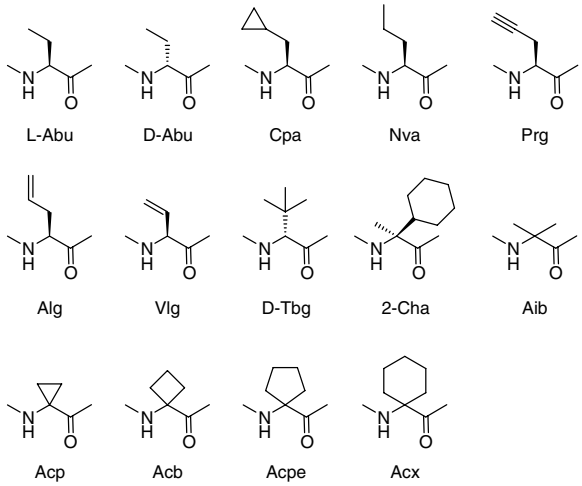

Figure 3. Structure of the non-natural amino acids in position 2 used in Table 2.

result in protection OXM from DPP-IV cleavage were therefore identified from analysis of prior SAR on DPP-IV-resistant GLP-1 analogs. In particular, based on the report that *N*-pyroglutamyl-GLP-1 and *N*-acetyl-GLP-1 are completely resistant to DPP-IV, albeit with somewhat reduced potency on GLP1R [20], we synthesized *N*-pyroglutamyl-OXM-NH_2 (Pyr-OXM-NH_2, **4**) and *N*-acetyl-OXM-NH_2 (Ac-OXM-NH_2, **5**) (Table 1). **4** is inactive on both receptors, while addition of Pyr had a strongly negative impact on GCGR activity, but less so on GLP1R. Moreover, unlike for GLP-1, the two modifications did not protect against DPP-IV proteolysis.

The exploration of *N*-capping groups was extended to Bz, Bzl, and PEG_4 (compounds **6–8**). The structure of all the capping groups explored is reported in Figure 2. Addition of either Bz or Bzl yielded DPP-IV-resistant analogs, active at both receptors: Bzl resulted in tenfold potency loss on both receptors, while Bz caused tenfold decrease in potency on GLP1R, but retained full activity on GCGR (Table 1). Capping with PEG_4 was detrimental to activity and did not provide any protection against DPP-IV.

For GLP-1, the presence of an intact *N*-terminal α-amino group is required for DPP-IV cleavage, and modifications of the *N*-terminal His can confer resistance to proteolysis [21]. Similar changes were explored in the context of OXM. Replacement of His with imidazole-lactic acid (Imi-H), which substitutes the *N*-terminal α-amino group with an hydroxyl (**9**) is compatible with activity at both receptors, with only threefold decreased potency, and confers stabilization against DPP-IV proteolysis (Figure 2 and Table 1). Also, *N*-methylation of the α-amino group confers protection against proteolysis for both the *N*-methylated and the *N,N*-dimethylated analogs Me-H-OXM-NH_2 (**10**) and Me_2-H-OXM-NH_2 (**11**). However, while the monomethylated analog (**10**) retains good potency on both receptors, the dimethylated analog (**11**) is completely inactive on GCGR and loses two orders of magnitude of potency on GLP1R. Removal of the α-amino group in the desamino-histidyl analog, ΔNH_2-H-OXM-NH_2 (**12**), confers optimal resistance against proteolysis with four- to eightfold decreased potency on the two receptors.

Overall, deletion of the *N*-terminal amine or substitution with OH or Me, all confer resistance to DPP-IV proteolysis, suggesting that for OXM, like for GLP-1, an intact *N*-terminal α-amino group is a critical determinant for susceptibility to DPP-IV.

Modifications at position 2

The recognized substrate sequence for DPP-IV is the *N*-terminal dipeptide Xaa–Yaa, with Y = Pro, Ala, or Ser. Thus, in addition to changes in the *N*-terminal amine, modification of the second amino acid has been pursued to obtain metabolically stable analogs of GLP-1 [22]. A similar approach was applied to OXM, with substitution of Ser^2 with a series of natural and non-natural amino acids (Figure 3 and Table 2). Most substitutions with natural amino acids are detrimental to activity, with the exception of the Ala^2 analog (**13**), which shows tenfold increased potency toward GLP1R. However, this analog shows 100-fold loss of potency on GCGR, and no resistance to DPP-IV. Gly^2 (**20**) is compatible with activation only at GLP1R, but remains a good substrate for DPP-IV. Both Ile (**22**) and Leu (**23**) instead yield analogs resistant to the enzyme, but with tenfold lower potency on GLP1R, and no activity on GCGR. Pro (**26**) maintains potency at GLP1R but not at GCGR, with no resistance to proteolysis.

Replacement of Ser^2 with D-amino acids, such as D-Ala (**31**), D-Ser (**32**), and D-Abu (**34**, Abu, aminobutyric acid) confers resistance to proteolysis. However, only the D-Ser^2 analog (**32**) remains a balanced agonist at both receptors, with only slightly decreased potency. The D-Ala^2 analog (**31**) loses activity on GCGR, while D-Abu^2 (**34**) shows tenfold lower potency on GLP1R and 100-fold lower on GCGR.

Substitution of Ser^2 with smaller aliphatic residues decreases protection from DPP-IV. In the series Abu (**33**), β-cyclopropyl-alanine (Cpa, **35**), norvaline (Nva, **36**), propargylglycine (Prg, **37**), and vinylglycine (Vlg, **39**) whose structures are shown in Figure 2, only Prg confers resistance to the enzyme. The Prg^2 analog maintains full activity on GLP1R, but is 100-fold less potent on GCGR.

Journal of PeptideScience

Table 2. List of OXM analogs with substitutions at position 2

Compound	Peptide[a]	EC_{50} (nM)[b] on GLP1R −DPP-IV	EC_{50} (nM)[b] on GLP1R +DPP-IV	EC_{50} (nM)[b] on GCGR
2	OXM-NH_2	9.2	>200	5.5
13	[Ala^2]-OXM-NH_2	0.2	227	94
14	[Arg^2]-OXM-NH_2	394	na	na
15	[Asn^2]-OXM-NH_2	124	180	na
16	[Asp^2]-OXM-NH_2	195	216	>800
17	[Glu^2]-OXM-NH_2	163	163	na
18	[Gln^2]-OXM-NH_2	123	171	na
19	[Phe^2]-OXM-NH_2	265	1031	na
20	[Gly^2]-OXM-NH_2	3.3	102	na
21	[His^2]-OXM-NH_2	300	429	na
22	[Ile^2]-OXM-NH_2	57	34	>300
23	[Leu^2]-OXM-NH_2	27	31	na
26	[Pro^2]-OXM-NH_2	9.5	>1000	>300
27	[Thr^2]-OXM-NH_2	87	500	24
28	[Trp^2]-OXM-NH_2	223	221	na
29	[Tyr^2]-OXM-NH_2	411	293	na
30	[Val^2]-OXM-NH_2	64	79	na
31	[D-Ala^2]-OXM-NH_2	5	7	310
32	[D-Ser^2]-OXM-NH_2	18	13	12
33	[Abu^2]-OXM-NH_2	45	1000	379
34	[D-Abu^2]-OXM-NH_2	72	68	188
35	[Cpa^2]-OXM-NH_2	144	329	na
36	[Nva^2]-OXM-NH_2	140	914	704
37	[Prg^2]-OXM-NH_2	7	58	437
38	[Alg^2]-OXM-NH_2	97	>500	na
39	[Vlg^2]-OXM-NH_2	139	117	158
40	[D-Tbg^2]-OXM-NH_2	40	53	>1000
41	[Cha^2]-OXM-NH_2	>500	>500	na
42	[Aib^2]-OXM-NH_2	0.5	0.4	68.6
43	[Acp^2]-OXM-NH_2	2.1	53	174
44	[Acb^2]-OXM-NH_2	0.2	21	9.7
45	[$Acpe^2$]-OXM-NH_2	100	107	161
46	[Acx^2]-OXM-NH_2	301	466	340

Agonist potency *in vitro* against GLP1R, with and without pre-incubation with DPP-IV, and against GCGR.
[a] Acp, 1-amino-1-cyclopropane carboxylic acid; Acb, 1-amino-1-cyclobutane carboxylic acid; Acpe, 1-amino-1-cyclopentane carboxylic acid; Acx, 1-amino-1-cyclohexane carboxylic acid; Alg, allylglycine; 2-Cha, 2-amino-2-cyclohexyl-propanoic acid; Cpa, β-cyclopropyl-alanine; Nva, aminovaleric acid; Prg, propargylglycine; Vlg, vinylglycine; D-Tbg, D-tert-butylglycine.
[b] na, not active.

Table 3. OXM analogs with modifications at position 3

Compound	Peptide[a]	EC_{50} (nM) on GLP1R −DPP-IV	EC_{50} (nM) on GLP1R +DPP-IV	EC_{50} (nM) on GCGR
1	OXM	7.0	>200	5.7
47	[Asp^3]-OXM-OH	3	42	>1000
48	[Glu^3]-OXM-OH	21	148	>1000
49	[Leu^3]-OXM-OH	40	148	>1000
50	[Nle^3]-OXM-OH	13	>200	>500
51	[Pro^3]-OXM-OH	770	670	>500

Agonist potency *in vitro* against GLP1R, with and without pre-incubation with DPP-IV, and against GCGR.
[a] Nle, norleucine.

The more bulky D-tert-butylglycine (D-tbg, **40**) and 2-amino-2-cyclohexyl-propanoic acid (Cha, **41**) analogs, although resistant to DPP-IV, show partial (**40**) or complete (**41**) loss of potency on GLP1R, and are inactive on GCGR.

Deacon *et al*. [22] had shown that replacement of the Ala^2 in GLP-1 with an α,α-disubstituted amino acid such as α-amino-isobutyric acid (Aib) confers resistance against proteolysis. The same is true for the OMX Aib^2 analog (**42**). This analog is a highly potent and selective GLP1R agonist, with tenfold lower potency on GCGR and tenfold *higher* potency on GLP1R. On the basis of this promising finding, position 2 substitutions were pursued with cyclic α-disubstituted amino acids of increasing ring size, from the smaller 3-membered ring 1-amino-1-cyclopropane carboxylic acid (Acp, **43**) to the largest 6-membered ring 1-amino-1-cyclohexane carboxylic acid (Acx, **46**). The optimal ring size was four: Acp confers some proteolytic resistance and maintains activity on GLP1R, but less so on GCGR. 1-Amino-1-cyclobutane carboxylic acid (Acb, **44**) confers some degree of resistance against proteolysis, maintains potency on GCGR, and is tenfold *more* potent on GLP1R. Larger cycles such as 1-amino-1-cyclopentane carboxylic acid (Acpe, **45**) and Acx (**46**) decreased activity on both receptors.

In summary, substitution of Ser in position 2 with D-Ser or Acb confers resistance to DPP-IV, and preserves a balanced GLP1R/GCGR dual agonist profile. Conversely, substitution of Ser^2 with D-Ala or Aib yields DPP-IV-resistant analogs with increased potency and selectivity toward GLP1R. The latter feature might be useful for the design of novel GLP-1 mimetics, and was further explored (see later).

Modifications at position 3

OXM analogs with selected modifications at position 3 are shown in Table 3. An acidic residue (Glu) is present at position 3 in GLP-1, exenatide, and PACAP, while OXM and GCG have Gln in that position. Substitution of Gln^3 with Asp (**47**) or Glu (**48**) dials out activity on GCGR, yielding an analog with complete selectivity toward GLP1R. Interestingly, also the substitution with Leu (**49**) and norleucine (Nle, **50**) yields GLP1R-selective analogs, while Pro (**51**) is detrimental to activity on both receptors.

In addition to showing complete selectivity, the Asp^3 analog **47** also shows increased potency and some degree of resistance to DPP-IV. However, this substitution generates an Asp^3–Gly^4 sequence, prone to aspartimide formation, and Glu^3 was therefore selected for further work (see later).

Combining modifications at positions 2 and 3

On the basis of the results of single amino acid substitutions, we prepared analogs with substitutions at both positions 2 and 3 (Table 4). The combination of Gly^2 and Glu^3 (**52**) yields complete selectivity toward GLP1R, as observed for the single-substitution Glu^3 analog **48**, and partial protection from DPP-IV cleavage. The combination of D-Ser^2 with either Asp^3 (**53**) or Glu^3 (**54**) yields potent, GLP1R-selective analogs with complete resistance to DPP-IV proteolysis. The combination of Aib^2 and Asp^3 (**55**) yields a GLP1R-selective, subnanomolar analog with complete resistance to DPP-IV. The Aib^2Glu^3 analog **56** is also DPP-IV-resistant and GLP1R-selective, but less potent.

Table 4. OXM analogs with modifications at positions 2 and 3

Compound	Peptide	EC_{50} (nM) on GLP1R −DPP-IV	EC_{50} (nM) on GLP1R +DPP-IV	EC_{50} (nM) on GCGR[a]
2	OXM-NH_2	9.2	>200	5.5
52	[Gly^2,Glu^3]-OXM-NH_2	5.4	51	na
53	[D-Ser^2,Asp^3]-OXM-NH_2	1.7	2	na
54	[D-Ser^2,Glu^3]-OXM-NH_2	3.4	6	na
55	[Aib^2,Asp^3]-OXM-NH_2	0.2	0.2	na
56	[Aib^2,Glu^3]-OXM-NH_2	1.0	1.5	na

Agonist potency *in vitro* against GLP1R, with and without pre-incubation with DPP-IV, and against GCGR.
[a] na, not active.

Overall, the results of the *N*-terminal substitutions are consistent with prior literature. In particular, Runge *et al*. had shown that substitution of the GLP-1 residues Ala^2 or Glu^3 into GCG was detrimental for GCGR binding [23]. By a domain-swapping mutagenesis strategy, the same authors identified the extracellular end of TM2 of the GCGR/GLP1R as the critical counterpart of the *N*-terminal sequence of the two hormones [23].

In addition to decreasing GCGR binding, Ala^2 in OXM considerably improves binding to GLP1R (**14**, Table 2). This might be due to stabilization of an α-helical structure. Accordingly, we found that the most GLP1R potency-enhancing substitutions in OXM were Aib and its cyclic analog Acb, (**42** and **44**, Table 2), which are also known helix nucleators/stabilizers [24]. By contrast, the structure of GCG/OXM when bound to GCGR may be more similar to the β-coil structure found for PACAP [19], which shares the conserved Ser at position 2. In the β-coil structure of PACP, Ser^2 is pointing away from the Ile^5–Phe^8–Tyr^{10} hydrophobic patch [19], and is possibly engaged in a H-bond: for OXM, we found Thr^2 as the only substitution compatible with GCGR activity (**27**, Table 1). Such interaction might be maintained by D-Ser with just small changes in the main chain dihedral angles; similar changes in PACAP have been suggested to drive the transition between the membrane-bound and the receptor-bound conformation [19]. By contrast, the $Ala^2 \rightarrow$ D-Ala^2 substitution would be more disruptive of the α-helical conformation required for GLP1R binding.

In summary, D-Ser^2 appeared the best residue to maintain activity at both receptors, while affording protection from DPP-IV cleavage, and was selected for our subsequent work.

Long-acting Analogs

The next intent was to identify compounds with improved half-life in circulation, due to reduced proteolytic degradation and/or reduced renal clearance. Derivatization with fatty acids has been successfully used to increase the half-life of GLP-1 analogs [25] and recently, acylated derivatives of OXM have been described which show efficacy up to 8 h post administration [16]. Alternatively, derivatization with cholesterol has also been proposed as a way to increase the half-life of peptides [26], while at the same time increasing the potency of the peptide ligand toward membrane receptors. The use of cholesterol for membrane targeting of a peptide has also been described to increase the potency of a transition-state β-secretase inhibitor [27].

We explored derivatization with cholesterol of the [D-Ser^2]-OXM-NH_2 analog at positions 20, 28, and 38 (**57–59**, Table 5). For this purpose we synthesized two bromo derivatives of cholesterol, cholest-5-en-3-yl bromoacetate (**60**) and cholest-5-en-3-yl-1-bromo-2-oxo-6,9,12,15-tetraoxa-3-azaoctadecan-18-oate**(61)** as shown in Figure 4. Cholesteroylation was accomplished by reaction of **60** or **61** with a Cys residue substituted in positions 20, 28, or 38 of the peptide, to produce peptides **59, 62**, and **63**, as shown in Figure 5.

While cholesterylation at positions 20 (**57**) and 28 (**58**) yielded inactive compounds, the introduction of a cholesterol group at the *C*-terminus was highly beneficial. **59** showed 100-fold improvement in potency on GLP1R with respect to the non-cholesterylated analog [D-Ser^2]-OXM-NH_2 (**32**), while the activity on the GCGR was unaltered. Introduction of a tetraethylene glycol (PEG) spacer between the *C*-terminal Cys and cholesterol further boosted potency tenfold, this time for both receptors: the resulting analog **62** showed dual GLP1R/GCGR agonism, with subnanomolar potency at both receptors.

The observed increase in potency by cholesterol derivatization may be due to the increased affinity of the peptide for membranes, and in particular for the lipid raft compartment, as shown for the antiviral peptide C34 [26], since it is known that GPCRs are also enriched in lipid rafts [28]. The increase in concentration at the receptor should enhance peptide potency, provided that the location of cholesterol within the molecule does not prevent the peptide from achieving its bioactive conformation. The recently published structure of GLP-1 in complex with the extracellular domain of the GLP1R [29] offers an explanation for the lack of activity of cholesterol derivatives at positions 20 and 28, as the native residues at these positions establish major contacts with the receptor. Interestingly, the derivative at position 28 – the *C*-terminus of the GCG sequence embedded in OXM – maintains some activity at the GCGR, further highlighting

Table 5. OXM analogs with incorporation of a cholesterol moiety

Compound	Peptide	Lipid	EC_{50} (nM)[a] on GLP1R −DPP-IV	EC_{50} (nM)[a] on GLP1R +DPP-IV	EC_{50} (nM)[a] on GCGR
2	OXM-NH_2		9.2	>200	5.5
32	[D-Ser^2]-OXM-NH_2		18	13	12
57	[D-Ser^2]-OXM-NH_2	C20(chol)	na	na	na
58	[D-Ser^2]-OXM-NH_2	C28(chol)	na	na	247
59	[D-Ser^2]-OXM-NH_2	C38(chol)	0.1	0.1	12
62	[D-Ser^2]-OXM-NH_2	C38(PEG_4-chol)	0.05	0.06	0.7
63	[D-Ser^2,Glu^3]-OXM-NH_2	C38(PEG_4-chol)	0.3	0.2	60

Agonist potency *in vitro* against GLP1R, with and without pre-incubation with DPP-IV, and against GCGR.
[a] na, not active

Journal of PeptideScience

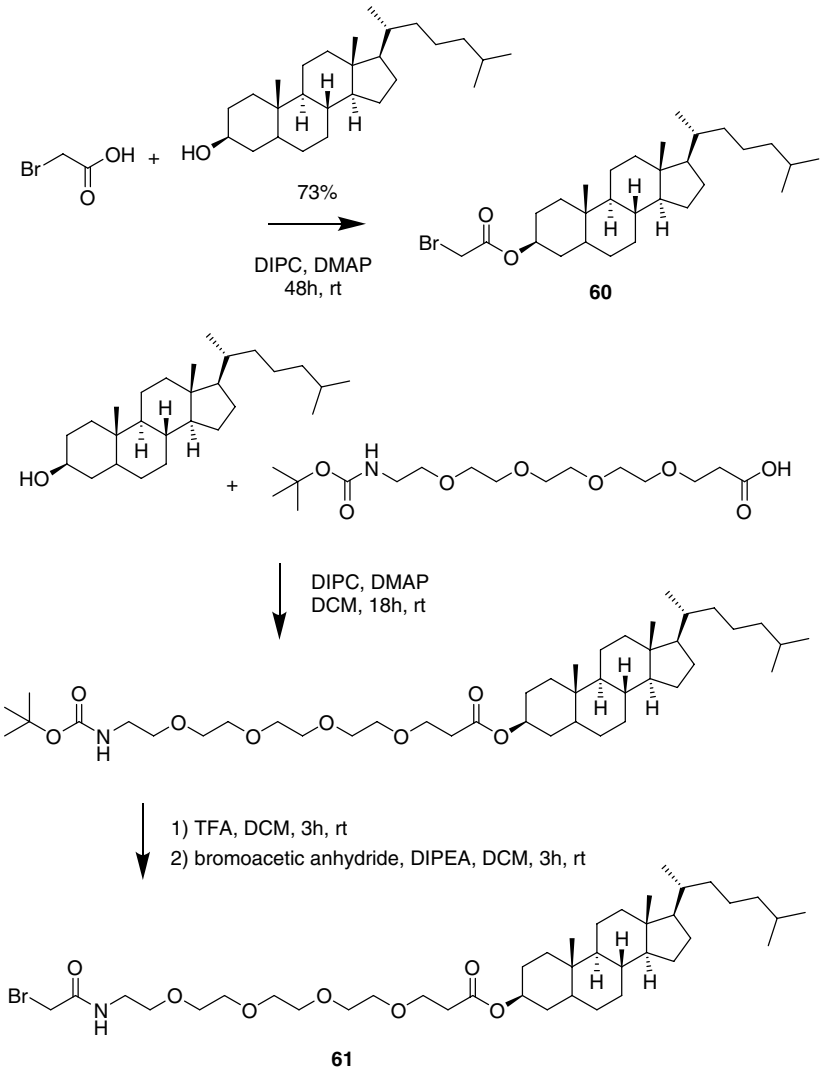

Figure 4. Synthesis of the cholesterol derivatives used in the synthesis of OXM analogs 56–59 and 62–63.

the importance of the GCG *C*-terminus in differentiating between GLP1R and GCGR binding. Position 38, at the *C*-terminal end of the 8-aa extension present in OXM, is likely removed enough from the contact region to be compatible with binding, particularly if it occurs through a two-step mechanism as proposed for other peptide hormones: step 1, binding to the membrane and step 2, navigation in the membrane plane to the receptor site [19,30–32]. Accordingly, addition of a PEG spacer further improves peptide potency (compare **59** with **62**).

The cholesteroylated dual agonist **62** was evaluated for its pharmacokinetic properties in mice. While as previously reported, OXM has a circulatory half-life of a few minutes, the half-life of **62** upon intravenous injection at the concentration of 3.5 mg/kg is 1.7 h (Figure 6). As apparent from the figure, the plasma concentration of **62** after 6 h was ~200 μM, i.e. several orders of magnitude higher than the IC_{50} on both GLP1R and GCGR, indicating that the peptide was suitable for the intended chronic diet-induced obese (DIO) mouse study with once every other day administration.

On the basis of the SAR established for the short-lived OXM analogs, substitution of the glutamine at position 3 with glutamic acid was performed to produce a 'matched' long-lasting GLP1R-selective agonist. As expected, compound **63** is 200-fold more potent on GLP1R (IC_{50} = 0.3 nM) than on GCGR (IC_{50} = 60 nM). Moreover, when the relative potency of **62** and **63** was compared on mouse receptors, we found that the pair was more closely matched: for mGLP1R, the IC_{50} values of the dual agonist **62** and the single agonist **63** were 3.4 and 1.7 nM, respectively, while for mGCGR the IC_{50} values were 0.5 and 208 nM, respectively. We can only speculate that the differential effect of cholesterol derivatization on the human and mouse GLP1R/GCGR is due to differences in the assembly of the receptor complexes at the membrane site, where the peptide is driven by the cholesterol moiety.

The matched pair **62**–**63** (Figure 7) enabled studies, described in detail in a separate study [18], which demonstrated dual agonistic activity at both GLP1R and GCGR, as displayed by the long-lasting OXM analog **62**, is advantageous over equipotent agonistic activity at GLP1R only, as displayed by **63**, for reduction in food intake, body weight, and adiposity. Importantly, matched GLP1R and GLP1R/GCGR dual agonists were equally effective in normalizing basal glucose levels and improving glucose tolerance.

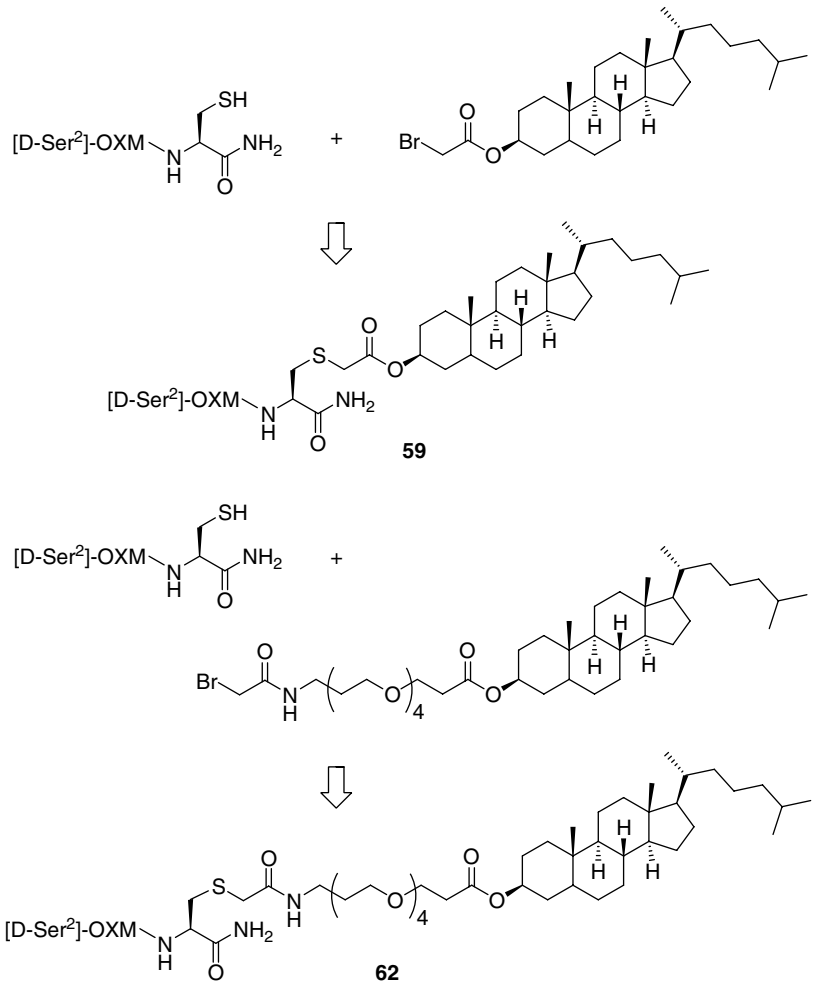

Figure 5. Synthesis of OXM analogs derivatized with cholesterol. Synthesis of analogs **59** and **62** (Table 4), where the cysteine residue is positioned at the *C*-terminus of the peptide (residue 38).

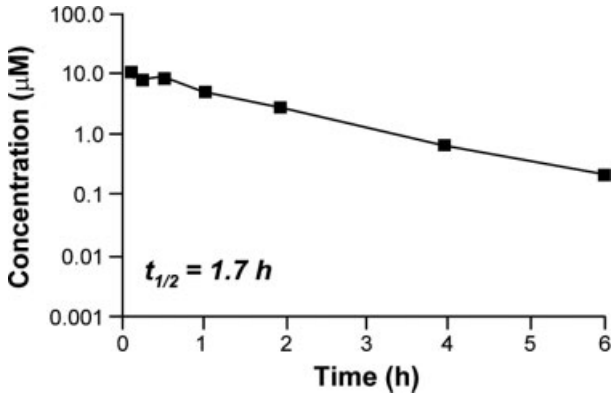

Figure 6. Pharmacokinetics of OXM analog **62** in mouse. Compound **62** was administered intravenously to C57BL/6 mice at 3.5 mg/kg in water, and the concentration monitored with time. The curve represents the mean of three animals. The calculated half-life is shown.

Conclusions

The SAR studies described herein yielded OXM-derived molecules that are resistant to DPP-IV degradation and display increased potency and duration of action with respect to the natural hormone, thus representing promising leads for the development of peptide therapeutics for the treatment of both obesity and diabetes. Moreover, a single substitution was identified, which can change the OXM pharmacological profile from a dual GLP1R/GCGR agonist to a selective GLP1R agonist. The latter finding enabled studies, described in detail in a separate manuscript [18], which highlight the potential of GLP1R/GCGR dual agonists as a superior class of therapeutics over the pure GLP1R agonists currently in clinical use, in agreement with the recent report by Day *et al.* [17]. On the basis of the clinical findings with OXM, i.e. the low observed incidence of treatment-associated nausea [12,13], one might expect that these agents may also confer the benefit of an improved tolerability profile.

Materials and Methods

Peptide Synthesis

Peptides were synthesized by solid-phase Fmoc chemistry with an APEX396 synthesizer (Advanced Chemtech, Louisville, KY, USA) using either a 1% cross-linked PEG–PS resin (Champion, Biosearch Technologies, Novato, CA, USA), or AM-Polysryrene LL resin (100–200 mesh, Novabiochem, Laufelfingen, CH), derivatized with the modified Rink linker p-[(R,S)-α-[9H-fluoren-9-yl-

Journal of PeptideScience

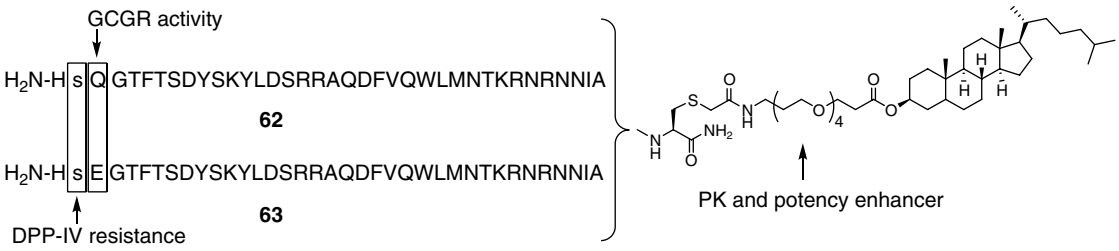

Figure 7. Matched pair of long-lasting OXM analogs. **62** is a dual GLP1R/GCGR agonist, **63** is a GLP1R-selective agonist.

methoxyformamido]-2,4-dimethoxybenzyl]-phenoxyacetic acid [33] for the peptides with *C*-terminal carboxyamide, and with a hydroxymethylphenoxyacetic linker for the peptides with a *C*-terminal carboxylate. The following side-chain protecting groups were used: OtBu for Asp and Glu; tBu for Ser, D-Ser, Thr, and Tyr; Boc for Lys and Trp; Trt for Asn, Cys, His, and Gln; Pbf for Arg.

All the amino acids were dissolved at 0.5 M concentration in a solution of 0.5 M HOBt in DMF, and activated with an equimolar amount of HBTU and a twofold molar excess of DIEA. Acylations were performed for 1 h with sixfold excess of activated amino acid over the resin amino groups. For compound **4**, Pyr was introduced at the end of the assembly by activation with equimolar amounts of DIPC and HOBt, using fourfold excess of activated reagent. Compound **5** was acetylated at the end of the assembly with tenfold excess of acetic anhydride in DMF. For compounds **6** and **7**, at the end of peptide assembly, threefold excess of Bzl–His or Bz–His, respectively, activated with equimolar amounts of HBTU and a twofold molar excess of DIEA, were reacted for 240 min (**6)** or overnight (**7**). For compound **8**, fourfold excess of m-dPEG$_4$®-acid (Quanta BioDesign, Powell, OH, USA) was activated with equimolar amounts of DIPC and HOBt. For compound **9**, fourfold excess was used of Imi-H activated with equimolar amounts of PyBOP, HOBt, and twofold molar excess of DIEA.

For compounds **10,11**, and **12**, threefold excess of Me–H, Me$_2$–H, or ΔNH$_2$–H were activated by reaction with equimolar amounts of HBTU and twofold molar excess of DIEA. The acylation reaction was performed for 3 h for **10** and**12** and overnight for **11**.

At the end of the synthesis, the dry peptide-resins, 1.3 g, were individually treated with 20 ml of the cleavage mixture, 88% TFA, 5% phenol, 2% triisopropylsilane, and 5% water [34] for 1.5 h at room temperature (rt). Cys-containing peptides were cleaved from the resins with 82.5% TFA, 5% phenol, 5% thioanisole, 2.5% ethandithiole, and 5% water for 1.5 h at rt. Each resin was filtered and the solution was added to cold methyl-*t*-butyl ether to precipitate the peptide. After centrifugation, the peptide pellets were washed with fresh cold methyl-*t*-butyl ether to remove the organic scavengers. The process was repeated twice. Final pellets were dried, resuspended in 20% acetonitrile in water, and lyophilized.

The crude peptides were purified by reverse-phase HPLC using preparative Waters RCM Delta-Pak™ C$_{-4}$, 300 Å cartridges (40 × 200 mm, 15 µm) and using as eluents (A) 0.1% TFA in water and (B) 0.1% TFA in acetonitrile. The following gradient of B was used: 20% isocratic (5 min), then 20–35% (20 min), flow rate 80 ml/min. Analytical HPLC was performed on a Phenomenex, Jupiter (CT, USA) C$_4$ 300 Å column (150 × 4.6 mm, 5 µm) or on a ACE 300 Å (150 × 4.6 mm, 3 µm, T = 45 °C) with the following gradient of B: 20% isocratic (5 min), 20–40% (20 min), 40–80% (3 min), flow rate 1 ml/min. The purified peptides were lyophilized, and structure and purity were confirmed by analytical HPLC and electrospray mass spectrometry on a Micromass LCZ platform. Analytical data for all the peptides are reported in Table 6.

Synthesis of Cholest-5-en-3-yl Bromoacetate (60)

A mixture of 100 mg of cholesterol and 40 mg of bromoacetic acid (1.1 eq) was dissolved in 10 ml of anhydrous DCM. Then 44 µl (1.1 eq) of DIPC and 1.5 mg (0.05 eq) of DMAP were added. The solution was left stirring at rt for 48 h and analyzed by TLC using as solvent 10 : 1 *n*-hexane/EtOAc. The solvent was evaporated and the reaction product was purified by silica gel flash chromatography in 1 : 1 *n*-hexane/DCM. The fractions containing the product were pooled, evaporated and lyophilized in water/acetonitrile 20 : 80. Yield: 73%.

NMR spectra were recorded on Bruker Avance spectrometer and acquired at 300 K. Proton chemical shifts are reported in parts per million (d) and are referenced to the residual proton signal of the deuterated solvent ($CDCl_3$ at 7.26 ppm). ^{1}H NMR (400 MHz; $CDCl_3$): δ 0.71 (s, 3H), 0.88 (d, J = 2.2 Hz, 3H), 0.90 (d, J = 2.2 Hz, 3H), 0.94 (d, J = 6.5 Hz, 3H), 0.96–1.72 (m, 21H), 1.06 (s, 3H), 1.81–2.08 (m, 5H), 2.38 (d, J = 7.7 Hz, 2H), 3.83 (s, 2H), 4.67–4.73 (m, 1H), 5.42 (d, 0.88 J = 3.4 Hz, 1H); *m/z* (ES$^+$) 508 (M+H).

Synthesis of Cholest-5-en-3-yl 1-bromo-2-oxo-6,9,12, 15-tetraoxa-3-azaoctadecan-18-oate (61)

1. *Synthesis of cholest-5-en-3-yl 2,2-dimethyl-4-oxo-3,8,11,14, 17-pentaoxa-5-azaicosan-20-oate.* *N*-t-boc-amido-dPEG$_4$®-acid (1 g, 2.7 mmol, Quanta BioDesign) was added to a solution of cholesterol (0.99 g, 2.7 mmol) in 40 ml of DCM, followed by DIPC (0.43 ml, 3.2 mmol) and DMAP (16 mg, 5%). The mixture was stirred at rt overnight and the solvent was evaporated under *in vacuo*. The crude was dissolved in EtOAc, washed with 1N HCl, saturated NH_4Cl and brine, dried over Na_2SO_4, filtered and concentrated. The crude was purified by flash column chromatography (BIOTAGE) on silica gel with a gradient 25–50% EtOAc in petroleum ether to afford 1.48 g of desired compound as colorless oil (Yield 75%).
2. *Synthesis of cholest-5-en-3-yl-1-bromo-2-oxo-6,9,12,15-tetraoxa-3-azaoctadecan-18-oate.* TFA (2 ml, 26 mmol) was added to a solution of the compound obtained in step 1 (1.48 g, 2 mmol) in 10 ml of DCM and the mixture was stirred at rt for 3 h. All the volatiles were removed under *in vacuo* and the crude was lyophilized to obtain a colorless oil that was dissolved in 60 ml of DCM. Bromoacetic anhydride (0.62 g, 2.4 mmol) was added followed by DIPEA (0.65 ml, 3.7 mmol) and the mixture was stirred at rt for 3 h. The solvent was removed under *in vacuo* and the crude purified by flash column chromatography on silica gel (BIOTAGE) with a gradient 50–90% EtOAc in petroleum ether to obtain 1.1 g of desired compound as a colorless oil (combined yield of the two steps, 74%); ^{1}H NMR

Table 6. Analytical characterization of the compounds used in this study

Compound	HPLC gradient[a]	Column[b]	RT (min)	Purity[c] (%)	MW found (Da)	MW calc (Da)
1	20–40%(20′)–80%(3′)	1	15.02	>95	4449.00	4449.80
2[d]	32–40%(20′)	2	11.34	>99	3482.80	3481.84
3	20–40%(20′)–80%(3′)	1	14.90	>95	4448.00	4447.94
4	20–40%(20′)–80%(3′)	1	12.53	>95	4559.00	4558.07
5	20–40%(20′)–80%(3′)	1	12.82	>95	4491.00	4490.98
6	20–40%(20′)–80%(3′)	1	13.19	>95	4553.00	4553.06
7	20–40%(20′)–80%(3′)	1	14.23	>95	4539.00	4539.07
8	20–40%(20′)–80%(3′)	1	12.87	>95	4667.00	4667.20
9	20–40%(20′)–80%(3′)	1	12.59	>97	4450.00	4449.93
10	20–40%(20′)–80%(3′)	1	12.32	>97	4463.00	4462.97
11	20–40%(20′)–80%(3′)	1	12.32	>95	4476.00	4477.00
12	20–40%(20′)–80%(3′)	1	12.60	>95	4434.00	4433.93
13	20–40%(20′)–80%(3′)	1	12.20	>95	4433.00	4432.91
14	20–40%(20′)–80%(3′)	1	11.90	>95	4519.00	4518.06
15	20–40%(20′)–80%(3′)	1	12.07	>95	4476.00	4475.97
16	20–40%(20′)–80%(3′)	1	12.39	>95	4476.00	4476.96
17	20–40%(20′)–80%(3′)	1	12.19	>95	4490.00	4490.98
18	20–40%(20′)–80%(3′)	1	12.07	>92	4489.00	4490.00
19	20–40%(20′)–80%(3′)	1	13.00	>95	4509.00	4509.05
20	20–40%(20′)–80%(3′)	1	12.53	>95	4418.73	4418.92
21	20–40%(20′)–80%(3′)	1	11.92	>95	4499.00	4499.01
22	20–40%(20′)–80%(3′)	1	12.77	>95	4474.82	4475.03
23	20–40%(20′)–80%(3′)	1	12.60	>95	4475.00	4475.03
24	20–40%(20′)–80%(3′)	1	12.14	>95	4489.00	4490.04
25	20–40%(20′)–80%(3′)	1	12.75	>90	4493.00	4493.07
26	20–40%(20′)–80%(3′)	1	12.49	>97	4459.00	4458.99
27	20–40%(20′)–80%(3′)	1	12.40	>95	4463.00	4462.97
28	20–40%(20′)–80%(3′)	1	13.22	>97	4548.00	4548.08
29	20–40%(20′)–80%(3′)	1	12.65	>95	4525.00	4525.05
30	20–40%(20′)–80%(3′)	1	16.28	>95	4462.00	4461.99
31	20–40%(20′)–80%(3′)	1	12.59	>95	4433.00	4433.93
32	20–40%(20′)–80%(3′)	1	12.22	>90	4449.00	4448.91
33	20–20%(5′)–35%(20′)–80%(3′)	3	20.72	>90	4446.00	4445.97
34	20–20%(5′)–35%(20′)–80%(3′)	3	20.82	>98	4445.30	4445.97
35	20–20%(5′)–35%(20′)–80%(3′)	3	21.22	>90	4471.40	4472.00
36	20–20%(5′)–35%(20′)–80%(3′)	3	21.07	>95	4459.80	4459.99
37	20–20%(5′)–35%(20′)–80%(3′)	3	20.94	>95	4455.60	4455.96
38	20–20%(5′)–35%(20′)–80%(3′)	3	19.07	>90	4458.00	4457.98
39	20–20%(5′)–35%(20′)–80%(3′)	3	21.66	>90	4444.50	4443.95
40	20–20%(5′)–35%(20′)–80%(3′)	3	19.40	>90	4474.60	4474.02
41	20–20%(5′)–35%(20′)–80%(3′)	3	23.67	>90	4513.40	4514.09
42	20–40%(20′)–80%(3′)	1	15.25	>90	4448.00	4446.97
43	20–20%(5′)–35%(20′)–80%(3′)	3	19.17	>90	4444.80	4443.95
44	20–20%(5′)–35%(20′)–80%(3′)	3	18.92	>90	4459.00	4457.98
45	20–20%(5′)–35%(20′)–80%(3′)	3	19.02	>90	4472.50	4472.00
46	20–20%(5′)–35%(20′)–80%(3′)	3	21.58	>95	4486.40	4486.03
47	20–40%(20′)–80%(3′)	1	12.74	>95	4435.00	4435.88
48	20–40%(20′)–80%(3′)	1	12.67	>95	4450.00	4449.91
49	20–40%(20′)–80%(3′)	1	13.42	>95	4434.00	4433.95
50	20–40%(20′)–80%(3′)	1	13.54	>95	4434.00	4433.95
51	20–40%(20′)–80%(3′)	1	12.75	>90	4418.00	4417.91
52	20–40%(20′)–80%(3′)	1	12.94	>95	4420.00	4419.91
53	20–35%(20′)–80%(3′)	1	14.72	>95	4435.32	4435.90
54	20–40%(20′)–80%(3′)	1	12.25	>95	4450.00	4449.93
55	20–35%(20′)–80%(3′)	1	14.89	>97	4433.52	4433.93
56	20–35%(20′)–80%(3′)	1	15.00	>97	4447.02	4447.96

Journal of PeptideScience

Table 6. (*Continued*)

Compound	HPLC gradient[a]	Column[b]	RT (min)	Purity[c] (%)	MW found (Da)	MW calc (Da)
57	40–60%(20′)–80%(3′)	3	10.55	>95	4849.00	4849.64
58	40–60%(20′)–80%(3′)	3	9.82	>95	4863.00	4863.67
59	40–60%(20′)–80%(3′)	3	12.97	>95	4978.60	4977.7
62	40–40%(5′)–60%(20′)–80%(3′)	3	21.00	>97	5226.00	5225.06
63	40–40%(5′)–60%(20′)–80%(3′)	3	20.97	>95	5226.36	5226.05

[a] Percentage of the B eluent.
[b] 1, Phenomenex Jupiter C_4 150 × 4.6 mm, 5 µm, 300 Å, 25 °C; 2, OPH RP-ODS C_{18} 250 × 4.6 mm 5 µm, 300 Å, 25 °C; 3, Ace C_4 150 × 4.6 mm 3 µm, 300 Å 45 °C.
[c] Estimated by HPLC.
[d] Product N#: 812345 Lot#: CG-04-00578, CPC Scientific Inc.

(300 MHz; $CDCl_3$): δ 0.67 (s, 3H), 0.87 (d, J = 6.5 Hz, 6H), 0.92 (d, J = 6.5 Hz, 3H), 0.96–1.69 (m, 21H), 1.02 (s, 3H), 1.75–2.08 (m, 5H), 2.32 (d, J = 7.7 Hz, 2H), 2.56 (t, J = 6.5 Hz, 2H), 3.45–3.54 (m, 2H), 3.56–3.71 (m, 14H), 3.79 (t, J = 6.5 Hz, 2H), 3.87 (s, 2H), 4.55–4.71 (m, 1H), 5.34–5.40 (m, 1H), 7.04–7.17 (m, 1H); *m/z* (ES^+) 755 (M+H).

Synthesis of Cholesteroylated Analogs

Compounds **57, 58, 59, 62**, and **63** were synthesized from the respective Cys-containing peptide precursors by conjugation via the thiol group of Cys with the bromoacetyl-cholesterol reagents **60** and **61**. In particular for compounds **57, 58**, and **59** the Cys-peptide precursor dissolved in DMSO was reacted with equimolar **60** dissolved in THF, followed by addition of 1% by volume of DIPEA; for compounds **62** and **63**, the Cys-peptide precursor dissolved in DMSO was reacted with 2.1 M excess of **61** dissolved in THF followed by addition of 3% by volume of DIPEA. In both cases, the reaction was complete after 30 min as assessed by HPLC–MS. The reaction was quenched by addition of TFA at a final pH of 4, and directly loaded on preparative reverse-phase HPLC using Waters RCM Delta-Pak™ C_4 300 Å cartridges (40 × 200 mm, 15 µm), using as eluents (A) 0.1% TFA in water and (B) 0.1% TFA in acetonitrile. The following gradient of eluent B was used: 40% isocratic (5 min) 40–55% (20 min), flow rate 80 ml/min. Analytical HPLC was performed on a ACE C_4 300 Å (150 × 4.6 mm, 3 µm, T = 45 °C) with the following gradient of eluent B: 40% isocratic (5 min) 40–60% B (20 min) 60–80% (3 min), flow rate 1 ml/min. The purified peptides were lyophilized, and structure and purity were confirmed by analytical HPLC and electrospray mass spectrometry on a Micromass LCZ platform. Analytical data for these peptides are reported in Table 6.

In Vitro Receptor Activation Assay

CHO cells were stably transfected with a mutant form of human GLP1R (Gly^3 → Ala, Ala^{460} → Gly) or human GCGR cloned into plasmid pIRES (Clontech, Mountain View, CA) as a fusion with green fluorescent protein (GFP), and grown to 80% confluency in sterile filtered F12 Nutrient Mixture (HAM) media containing 10% FBS, 1.0% penicillin–streptomycin, and 1.0 g of geneticin. Cells were washed briefly with PBS, dissociated with Cellstripper (Mediatech Inc., Herndon, VA), and resuspended in assay buffer (serum free) containing F12, 0.1% BSA, 100 µM RO 20–1724 at a density of 0.5 × 10^6 cell/ml. The cAMP HTRF kit calibration curve was prepared following the manufacturers protocol (CIS Bio International, France). For tested peptides a 100 µM solution was made in DMSO, and fourfold serial dilutions were made using assay buffer, in a 96-well plate. To a separate 96-well plate, 40 µl of cell suspension was added, followed by 10 µl diluted compound. The plate was covered and shaken gently for 30 min. Twenty-five microliters of each concentration of cAMP calibration curve and 25 µl of diluent were added to standard wells only and 25 µl of diluted cAMP XL-665 to all wells, followed by 25 µl diluted anti-cAMP cryptate conjugate. The plate was covered and incubated for 1 h at rt with gentle shaking. Increasing cAMP levels were determined by a decrease in TR-FRET signal as measured in an EnVision counter (PerkinElmer, Waltham, MA) in comparison to a standard curve of cAMP as per manufacturer's instructions.

In Vitro Stability to DPP-IV

To determine the stability of the peptides to cleavage by DPP-IV, a 5 µM solution of each peptide in 10 mM HEPES, 0.05 mg/ml BSA was incubated with 10 nM recombinant soluble human DPP-IV at 37 °C for 24 h before assaying for *in vitro* potency against GLP1R. Data were analyzed using the linear and nonlinear regression analysis software, GraphPad Prism (GraphPad Software Inc., San Diego, CA).

Pharmacokinetic Analysis of OXM Analog 62

The OXM analog **62** dissolved in water was administered to C57BL/6 mice (n = 3) at the concentration of 3.5 mg/kg, and the concentration of peptide was monitored with time using the *in vitro* cell-based cAMP bio-assay for GLP1R agonist potency. CHO cells stably transfected with human GLP1R were used to determine peptide concentrations by comparing the degree of cAMP accumulation in plasma samples from treated animals against a cAMP standard curve generated by spiking peptide standards into mouse plasma. The calculated pharmacokinetic parameters are: Cl_p (ml/min/kg): 0.7; Vd_{ss} (L/kg): 0.1; $t_{1/2}$ (h): 1.7.

Acknowledgements

The authors gratefully acknowledge Gennaro Ciliberto, Nancy Thornberry, and Bei B. Zhang for continuous support and discussions throughout this work. We also thank Marialuisa Rios Candelore, Maria Verdirame, Francesca Rech, and Silvia Pesci, for help with the experiments.

References

1 Drucker DJ, Buse JB, Taylor K, Kendall DM, Trautmann M, Zhuang D, Porter L. Exenatide once weekly versus twice daily for the treatment of type 2 diabetes: a randomised, open-label, non-inferiority study. *Lancet* 2008; **372**: 1240–1250.

2 Knop FK, Vilsboll T, Larsen S, Madsbad S, Holst JJ, Krarup T. No hypoglycemia after subcutaneous administration of glucagon-like peptide-1 in lean type 2 diabetic patients and in patients with diabetes secondary to chronic pancreatitis. *Diabetes Care* 2003; **26**: 2581–2587.

3 Drucker DJ, Dritselis A, Kirkpatrick P. Liraglutide. *Nat. Rev. Drug Discov.* 2010; **9**: 267–268.

4 Holst JJ. Enteroglucagon. *Annu. Rev. Physiol.* 1997; **59**: 257–271.

5 Baldissera FG, Holst JJ, Knuhtsen S, Hilsted L, Nielsen OV. Oxyntomodulin (glicentin-(33–69)): pharmacokinetics, binding to liver cell membranes, effects on isolated perfused pig pancreas, and secretion from isolated perfused lower small intestine of pigs. *Regul. Pept.* 1988; **21**: 151–166.

6 Gros L, Thorens B, Bataille D, Kervran A. Glucagon-like peptide-1-(7–36) amide, oxyntomodulin, and glucagon interact with a common receptor in a somatostatin-secreting cell line. *Endocrinology* 1993; **133**: 631–638.

7 Dakin CL, Gunn I, Small CJ, Edwards CM, Hay DL, Smith DM, Ghatei MA, Bloom SR. Oxyntomodulin inhibits food intake in the rat. *Endocrinology* 2001; **142**: 4244–4250.

8 Baggio LL, Huang Q, Brown TJ, Drucker DJ. Oxyntomodulin and glucagon-like peptide-1 differentially regulate murine food intake and energy expenditure. *Gastroenterology* 2004; **127**: 546–558.

9 Maida A, Lovshin JA, Baggio LL, Drucker DJ. The glucagon-like peptide-1 receptor agonist oxyntomodulin enhances beta-cell function but does not inhibit gastric emptying in mice. *Endocrinology* 2008; **149**: 5670–5678.

10 Dakin CL, Small CJ, Park AJ, Seth A, Ghatei MA, Bloom SR. Repeated ICV administration of oxyntomodulin causes a greater reduction in body weight gain than in pair-fed rats. *Am. J. Physiol. Endocrinol. Metab.* 2002; **283**: E1173–E1177.

11 Dakin CL, Small CJ, Batterham RL, Neary NM, Cohen MA, Patterson M, Ghatei MA, Bloom SR. Peripheral oxyntomodulin reduces food intake and body weight gain in rats. *Endocrinology* 2004; **145**: 2687–2695.

12 Wynne K, Park AJ, Small CJ, Patterson M, Ellis SM, Murphy KG, Wren AM, Frost GS, Meeran K, Ghatei MA, Bloom SR. Subcutaneous oxyntomodulin reduces body weight in overweight and obese subjects: a double-blind, randomized, controlled trial. *Diabetes* 2005; **54**: 2390–2395.

13 Wynne K, Park AJ, Small CJ, Meeran K, Ghatei MA, Frost GS, Bloom SR. Oxyntomodulin increases energy expenditure in addition to decreasing energy intake in overweight and obese humans: a randomised controlled trial. *Int. J. Obes. (Lond.)* 2006; **30**: 1729–1736.

14 Kervran A, Dubrasquet M, Blache P, Martinez J, Bataille D. Metabolic clearance rates of oxyntomodulin and glucagon in the rat: contribution of the kidney. *Regul. Pept.* 1990; **31**: 41–52.

15 Zhu L, Tamvakopoulos C, Xie D, Dragovic J, Shen X, Fenyk-Melody JE, Schmidt K, Bagchi A, Griffin PR, Thornberry NA, Sinha Roy R. The role of dipeptidyl peptidase IV in the cleavage of glucagon family peptides: in vivo metabolism of pituitary adenylate cyclase activating polypeptide-(1–38). *J. Biol. Chem.* 2003; **278**: 22418–22423.

16 Druce MR, Minnion JS, Field BC, Patel SR, Shillito JC, Tilby M, Beale KE, Murphy KG, Ghatei MA, Bloom SR. Investigation of structure-activity relationships of Oxyntomodulin (Oxm) using Oxm analogs. *Endocrinology* 2009; **150**: 1712–1722.

17 Day JW, Ottaway N, Patterson JT, Gelfanov V, Smiley D, Gidda J, Findeisen H, Bruemmer D, Drucker DJ, Chaudhary N, Holland J, Hembree J, Abplanalp W, Grant E, Ruehl J, Wilson H, Kirchner H, Lockie SH, Hofmann S, Woods SC, Nogueiras R, Pfluger PT, Perez-Tilve D, DiMarchi R, Tschop MH. A new glucagon and GLP-1 co-agonist eliminates obesity in rodents. *Nat. Chem. Biol.* 2009; **5**: 749–757.

18 Pocai A, Carrington PE, Adams JR, Wright M, Eiermann G, Zhu L, Du X, Petrov A, Lassman ME, Jiang G, Liu F, Miller C, Tota LM, Zhou G, Zhang X, Sountis MM, Santoprete A, Capitò E, Chicchi GG, Thornberry N, Bianchi E, Pessi A, Marsh DJ, SinhaRoy R. Glucagon-like peptide 1/glucagon receptor dual agonism reverses obesity in mice. *Diabetes* 2009; **58**: 2258–2266.

19 Inooka H, Ohtaki T, Kitahara O, Ikegami T, Endo S, Kitada C, Ogi K, Onda H, Fujino M, Shirakawa M. Conformation of a peptide ligand bound to its G-protein coupled receptor. *Nat. Struct. Biol.* 2001; **8**: 161–165.

20 Green BD, Mooney MH, Gault VA, Irwin N, Bailey CJ, Harriott P, Greer B, O'Harte FP, Flatt PR. N-terminal His(7)-modification of glucagon-like peptide-1(7–36) amide generates dipeptidyl peptidase IV-stable analogues with potent antihyperglycaemic activity. *J. Endocrinol.* 2004; **180**: 379–388.

21 Gallwitz B, Ropeter T, Morys-Wortmann C, Mentlein R, Siegel EG, Schmidt WE. GLP-1-analogues resistant to degradation by dipeptidyl-peptidase IV in vitro. *Regul. Pept.* 2000; **86**: 103–111.

22 Deacon CF, Knudsen LB, Madsen K, Wiberg FC, Jacobsen O, Holst JJ. Dipeptidyl peptidase IV resistant analogues of glucagon-like peptide-1 which have extended metabolic stability and improved biological activity. *Diabetologia* 1998; **41**: 271–278.

23 Runge S, Gram C, Bräuner-Osborne H, Madsen K, Knudsen LB, Wulff BS. Three distinct epitopes on the extracellular face of the glucagon receptor determine specificity for the glucagon amino terminus. *J. Biol. Chem.* 2003; **278**: 28005–28010.

24 Mahalakshmi R, Balaram P. Non-protein amino acids in the design of secondary structure scaffolds. *Methods Mol. Biol.* 2006; **340**: 71–94.

25 Madsen K, Knudsen LB, Agersoe H, Nielsen PF, Thogersen H, Wilken M, Johansen NL. Structure-activity and protraction relationship of long-acting glucagon-like peptide-1 derivatives: importance of fatty acid length, polarity, and bulkiness. *J. Med. Chem.* 2007; **50**: 6126–6132.

26 Ingallinella P, Bianchi E, Ladwa NA, Wang Y-J, Hrin R, Veneziano M, Bonelli F, Ketas TJ, Moore JP, Miller MD, Pessi A. Addition of a cholesterol group to an HIV-1 peptide fusion inhibitor dramatically increases its antiviral potency. *Proc. Natl. Acad. Sci. USA* 2009; **106**: 5801–5806.

27 Rajendran L, Schneider A, Schlechtingen G, Weidlich S, Ries J, Braxmeier T, Schwille P, Schulz JB, Schroeder C, Simons M, Jennings G, Knolker HJ, Simons K. Efficient inhibition of the Alzheimer's disease beta-secretase by membrane targeting. *Science* 2008; **320**: 520–523.

28 Chini B, Parenti M. G-protein coupled receptors in lipid rafts and caveolae: how, when and why do they go there?. *J. Mol. Endocrinol.* 2004; **32**: 325–338.

29 Underwood CR, Garibay P, Knudsen LB, Hastrup S, Peters GH, Rudolph R, Reedtz-Runge S. Crystal structure of glucagon-like peptide-1 in complex with the extracellular domain of the glucagon-like peptide-1 receptor. *J. Biol. Chem.* 2010; **285**: 723–730.

30 Bader R, Zerbe O. Are hormones from the neuropeptide Y family recognized by their receptors from the membrane-bound state? *ChemBiochem* 2005; **6**: 1520–1534.

31 Schwyzer R. Membrane-assisted molecular mechanism of neurokinin receptor subtype selection. *EMBO J.* 1987; **6**: 2255–2259.

32 Seelig A, Alt T, Lotz S, Holzemann G. Binding of substance P agonists to lipid membranes and to the neurokinin-1 receptor. *Biochemistry* 1996; **35**: 4365–4374.

33 Rink H. Solid-phase synthesis of protected peptide fragments using a trialkoxy-diphenyl-methylester resin. *Tetrahedron Lett.* 1987; **28**: 3787–3789.

34 Sole NA, Barany G. Optimization of solid-phase synthesis of [Ala8]-dynorphin A. *J. Org. Chem.* 1992; **57**: 5399–5403.

